Transient quantum transport in double-dot Aharonov-Bohm interferometers

Matisse Wei-Yuan Tu and Wei-Min Zhang*
Department of Physics, National Cheng Kung University, Tainan 70101, Taiwan

Jinshuang Jin
Department of Physics, Hangzhou Normal University, Hangzhou 310036, China

O. Entin-Wohlman† and A. Aharony‡
Physics Department, Ben Gurion University, Beer Sheva 84105, Israel

(Received 3 May 2012; revised manuscript received 26 July 2012; published 28 September 2012)

Real-time nonequilibrium quantum dynamics of electrons in double-dot Aharonov-Bohm (AB) interferometers is studied using an exact solution of the master equation. The building of the coherence between the two electronic paths shows up via the time-dependent amplitude of the AB oscillations in the transient transport current and can be enhanced by varying the applied bias on the leads, the on-site energy difference between the dots and the asymmetry of the coupling of the dots to the leads. The transient oscillations of the transport current do not obey phase rigidity. The circulating current has an antisymmetric AB oscillation in the flux. The nondegeneracy of the on-site energies and the finite bias cause the occupation in each dot to have an arbitrary flux dependence as the coupling asymmetry is varied.

DOI: 10.1103/PhysRevB.86.115453 PACS number(s): 73.23.−b, 73.63.−b

I. INTRODUCTION

Coherence of electronic transport through mesoscopic junctions has been studied intensively in nanoelectronic systems. In particular, the interference of electron waves has been visualized in Aharonov-Bohm (AB) interferometers via the AB oscillations of the conductance of a ring placed between two leads. Following the electron injection from the leads into the ring, the electrons undergo a nonequilibrium transport process before a steady interference pattern is reached. While the steady-state AB interference has been largely explored in the literature, the real-time dynamics of electronic transport in AB interferometers has not yet been fully understood. In this paper we study this dynamics in double-quantum-dot AB interferometers addressing the transient AB interference under various tunable parameters of the system.

The study of the wavy nature of electronic transmissions has been mainly focused on the complex amplitudes of the transmitted electrons in the scattering approach.[1,2] The archetype model contains a single quantum dot sitting on one of the two arms of the AB ring. A quantum point contact (QPC) placed nearby the quantum dot has been used to study the effect of a which-path detection.[3] A single-dot AB interferometer has been realized in a closed geometry[4] and also in an open one.[5] Phase rigidity in a two-terminal geometry has been experimentally discovered[4,6] and theoretically explained.[7] The effect of electron-electron interactions on transport through AB interferometers has also been explored.[8,9] A review on the early progress can be found in Ref. 10. Extracting the transmission phase from the AB oscillations is another main issue. The way continuous phase shifts (as opposed to phase rigidity) of the AB oscillations can be induced by breaking the unitarity of the scattering matrix and the way such phase shifts depend on the properties of electron losses have been investigated.[11,12] Likewise, ways of extracting both the amplitude and the phase of the intrinsic transmission amplitude from the measured conductance without opening the interferometer have been suggested.[13] The studies of AB interferometers with two quantum dots placed on the two arms of the ring have been focused on different issues, such as the flux-dependent level attraction,[14] the effect of intradot and interdot Coulomb interactions,[15–17] inelastic scattering with phonons,[18] as well as extracting transmission phases from the current measurements using QPC placed next to the one of the quantum dots.[19]

The above investigations are concentrated mainly on steady-state properties of quantum-dot AB interferometers. Recently, time-dependent and transient transport through mesoscopic systems have attracted considerable interest. Thus, transient effects on an Anderson impurity,[20] in the Kondo regime,[21] and on correlated quantum dots, exploiting the renormalization-group approach,[22] have been considered. Dissipation in the nonequilibrium spin-fermion problem has been analyzed, also for AB interferometers, using a path-integral formulation.[23] In this paper we consider a double-quantum-dot AB interferometer as sketched in Fig. 1, where a single active charge state on each dot is assumed and electron-electron interactions are ignored. In a recent work,[24] some of us have studied the electron dynamics in this system under the condition of identical on-site energies of the dots and symmetric couplings to the leads. In that study, a phase localization phenomenon has been found. This phenomenon has also been confirmed by the exact numerical path-integral method in which electron-electron interactions are also included.[23] In the present paper, we systematically explore the general transient transport dynamics with nonidentical on-site energies on the dots and asymmetric couplings to the left and the right leads (but not between the two dots). In particular, besides the search for the dynamical flux dependencies of the transient net current, we also examine the flux dependence of the transient electronic occupation in each dot and the transient circulating current. The electronic occupation on each dot can be measured in experiments and contains rich information about the transport processes. The relatively large circulating current at zero or small bias may provide new insights into electron coherence during the transport.

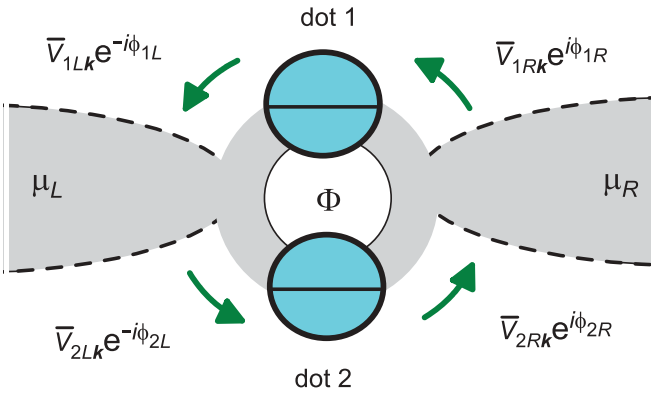

FIG. 1. (Color online) A schematic sketch of the system. The AB interferometer, consisting of two single-level dots, is connected to a source and a drain set at different chemical potentials, μ_L and μ_R, respectively. The interferometer is threaded by a magnetic flux Φ measured in units of the flux quantum $\Phi_0 = hc/e$.

Here is a summary of the main results we obtain. By setting the two electronic leads (as the reservoirs) at thermal equilibrium initially with no excess electrons on the double dot, we monitor the time evolutions of the electronic charge occupation, the transport net current, and the circulating current. When the two on-site energies on the dots are identical (namely the double dot is degenerate), regardless of the coupling asymmetry to the leads, we find that the total electronic occupation on the double dot and the net current are always symmetric in the flux, while the occupation difference between the two dots and the circulating current are always antisymmetric in it. We also find that the times needed for the total occupation to reach its steady-state values are much longer near zero flux, compared with the case where the flux value is away from zero. By breaking the degeneracy of the double dot, the net current is allowed to break phase rigidity transiently at any bias. The flux dependence of the total occupation number changes arbitrarily as the coupling asymmetry is varied at finite biases. The nondegenerate double dot coupled asymmetrically to the leads also drives the circulating current slightly away from an antisymmetric flux dependence immediately after the current is switched on, but it then quickly becomes completely antisymmetric in the flux.

The rest of the paper is organized as follows. In Sec. II we outline the basic formalism describing the nonequilibrium electronic dynamics for nanoelectronic devices in general and for the double-dot AB interferometer in particular. In Sec. III we present analytical expressions for the electronic occupations, the transient net current, and the circulating current. In Sec. IV and the Appendix we consider the steady-state limit, reproduce known results for this system, and compare them with ours. In Sec. V we numerically demonstrate the transient flux dependence of the electronic occupations and currents. Finally, conclusions are drawn in Sec. VI.

II. BASIC FORMALISM

In this section we give a brief introduction to the nonequilibrium quantum theory that can describe transient quantum transport and quantum coherence in nanoelectronic systems[25,26] and then apply it to the double-quantum-dot AB interferometer considered in this paper.

The Hamiltonian of the prototypical nanoelectronic system we consider can be written as

$$\mathcal{H} = \mathcal{H}_{\rm s} + \mathcal{H}_{\rm E} + \mathcal{H}_{\rm T}, \tag{1}$$

where $\mathcal{H}_{\rm s} = \sum_{ij} E_{ij} a_i^\dagger a_j$ is the Hamiltonian of the central system with i,j labeling the electronic levels in the dots, $\mathcal{H}_{\rm E} = \sum_{\alpha \boldsymbol{k}} \epsilon_{\alpha \boldsymbol{k}} c_{\alpha \boldsymbol{k}}^\dagger c_{\alpha \boldsymbol{k}}$ is the lead Hamiltonian with α labeling the leads, $\boldsymbol{k}$ denoting the states in the leads, and $\mathcal{H}_{\rm T} = \sum_{i\alpha \boldsymbol{k}} [V_{i\alpha \boldsymbol{k}} c_{\alpha \boldsymbol{k}}^\dagger a_i + {\rm H.c.}]$ describing the tunneling between the dots and the leads. Here $a_i^\dagger$ (a_i) and $c_{\alpha \boldsymbol{k}}^\dagger (c_{\alpha \boldsymbol{k}})$ are the electron creation (annihilation) operators for electronic levels i and $\boldsymbol{k}$ in the dots and in lead α, respectively. $E_{ii} = E_i$ is the energy of level i, $E_{ij} (i \neq j)$ is the tunneling amplitude between the different levels in the dots, and $V_{i\alpha k}$ is the tunneling amplitude between the dots and the leads. Electron-electron interactions are ignored.

Since the central system is open to the electron reservoirs (via the leads), its nonequilibrium dynamics is naturally described by the reduced density matrix $\rho(t)$ which is defined by tracing over the states of the leads,

$$\rho(t) = {\rm tr}_{\rm E} \rho_{\rm tot}(t) = {\rm tr}_{\rm E}[e^{-i\mathcal{H}(t-t_0)} \rho_{\rm tot}(t_0) e^{i\mathcal{H}(t-t_0)}], \tag{2}$$

where $\rho_{\rm tot}(t)$ is the total density matrix of the central system plus the leads. Electronic occupations on the discrete electronic states in the dots can be read from $\rho(t)$. The electronic transport through the central system is characterized by the currents flowing from the leads into the dots, defined by $I_\alpha = -e\frac{d}{dt}\sum_{\boldsymbol{k}\in\alpha} {\rm tr}_{\rm tot}[c_{\alpha \boldsymbol{k}}^\dagger c_{\alpha \boldsymbol{k}} \rho_{\rm tot}(t)]$ for lead α. This can be further decomposed into separate contributions through each dot:

$$I_\alpha = \sum_i I_{i\alpha}, \quad I_{i\alpha} = ie \sum_{\boldsymbol{k}\in\alpha} {\rm tr}_{\rm tot}[V_{i\alpha \boldsymbol{k}} c_{\alpha \boldsymbol{k}}^\dagger a_i \rho_{\rm tot}(t) - {\rm H.c.}]. \tag{3}$$

In Eqs. (2) and (3), ${\rm tr}_E$ and ${\rm tr}_{\rm tot}$ denote the traces over the states of the leads and the total system, respectively. Throughout the paper, we use units in which $\hbar = 1$.

As usual, we assume[27] that the central dot system is initially decoupled from the leads, and the leads are initially at thermal equilibrium with the chemical potential μ_α and inverse temperature $\beta = 1/k_B T$ for lead α, whose Fermi distribution function is given by $f_\alpha(\epsilon) = 1/[e^{\beta(\epsilon-\mu_\alpha)} + 1]$. Then the exact equations governing the time evolution of the reduced density matrix and the transient currents are[25,26]

$$\frac{d}{dt}\rho(t) = -i[\mathcal{H}_{\rm s}, \rho(t)] + \sum_{i\alpha} [\mathcal{L}_{i\alpha}^+(t) + \mathcal{L}_{i\alpha}^-(t)]\rho(t), \tag{4a}$$

$$I_{i\alpha}(t) = e{\rm tr}_{\rm s}[\mathcal{L}_{i\alpha}^+(t)\rho(t)] = -e{\rm tr}_{\rm s}[\mathcal{L}_{i\alpha}^-(t)\rho(t)], \tag{4b}$$

where the superoperators $\mathcal{L}_{i\alpha}^\pm(t)$ are expressed explicitly by

$$\begin{aligned}
\mathcal{L}_{i\alpha}^+(t)\rho(t) = &-\sum_j \{\lambda_{\alpha ij}(t)[a_i^\dagger a_j \rho(t) + a_i^\dagger \rho(t) a_j] \\
&+ \kappa_{\alpha ij}(t) a_i^\dagger a_j \rho(t) + {\rm H.c.}\}, \\
\mathcal{L}_{i\alpha}^-(t)\rho(t) = &\sum_j \{\lambda_{\alpha ij}(t)[a_j \rho(t) a_i^\dagger + \rho(t) a_j a_i^\dagger] \\
&+ \kappa_{\alpha ij}(t) a_j \rho(t) a_i^\dagger + {\rm H.c.}\},
\end{aligned} \tag{5}$$

and tr_s is the trace over the states of the dots. The first term on the right-hand side of Eq. (4a) is the renormalized Liouville operator of the central dot system. The second and the third terms, expressed in terms of the superoperators, are nonunitary. The nonunitarity is induced by electronic dissipation and fluctuation processes due to the couplings of the central dot system to the electronic reservoirs. The transient transport current is determined from the nonunitary dynamics, as shown by Eq. (4b). Equations (4) and (5) form the basis of the nonequilibrium description of quantum coherence and quantum transport in mesoscopic systems.

The time-dependent dissipation and fluctuation coefficients in Eqs. (5), $\boldsymbol{\kappa}_\alpha(t)$ and $\boldsymbol{\lambda}_\alpha(t)$, respectively, are explicitly determined by the nonequilibrium retarded and correlation Green's functions of the dot system, denoted here by $\boldsymbol{u}(t)$ and $\boldsymbol{v}(t)$, respectively,[26] via the relations

$$\boldsymbol{\kappa}_\alpha(t) = \int_{t_0}^{t} d\tau\, \boldsymbol{g}_\alpha(t,\tau)\boldsymbol{u}(\tau)\boldsymbol{u}^{-1}(t), \tag{6a}$$

$$\boldsymbol{\lambda}_\alpha(t) = \int_{t_0}^{t} d\tau\{\boldsymbol{g}_\alpha(t,\tau)\boldsymbol{v}(\tau) - \widetilde{\boldsymbol{g}}_\alpha(t,\tau)\bar{\boldsymbol{u}}(\tau)\} - \boldsymbol{\kappa}_\alpha(t)\boldsymbol{v}(t). \tag{6b}$$

The nonequilibrium retarded and correlation Green's functions of the dot system obey the following dissipation-fluctuation integro-differential equations of motion

$$\frac{d}{dt}\boldsymbol{u}(\tau) + i\boldsymbol{E}\boldsymbol{u}(\tau) + \int_{t_0}^{\tau} d\tau'\boldsymbol{g}(\tau-\tau')\boldsymbol{u}(\tau') = 0, \tag{7a}$$

$$\frac{d}{dt}\boldsymbol{v}(\tau) + i\boldsymbol{E}\boldsymbol{v}(\tau) + \int_{t_0}^{\tau} d\tau'\boldsymbol{g}(\tau-\tau')\boldsymbol{v}(\tau') = \int_{t_0}^{t} d\tau'\widetilde{\boldsymbol{g}}(\tau-\tau')\bar{\boldsymbol{u}}(\tau'), \tag{7b}$$

subject to the conditions $\boldsymbol{u}(t_0) = I, \boldsymbol{v}(t_0) = 0$ with $t_0 \leqslant \tau \leqslant t$, and $\bar{\boldsymbol{u}}(\tau) = \boldsymbol{u}^\dagger(t-\tau+t_0)$ is the advanced Green's function. Here $\boldsymbol{E}$ is the on-site energy matrix of the dot system and $\boldsymbol{g} = \sum_\alpha \boldsymbol{g}_\alpha$ and $\tilde{\boldsymbol{g}} = \sum_\alpha \widetilde{\boldsymbol{g}}_\alpha$ are the self-energy corrections due to the coupling to the leads:

$$\boldsymbol{g}_\alpha(\tau) = \int \frac{d\omega}{2\pi}\boldsymbol{\Gamma}_\alpha(\omega)e^{-i\omega\tau}, \tag{8a}$$

$$\widetilde{\boldsymbol{g}}_\alpha(\tau) = \int \frac{d\omega}{2\pi} f_\alpha(\omega)\boldsymbol{\Gamma}_\alpha(\omega)e^{-i\omega\tau}. \tag{8b}$$

The spectral density $\boldsymbol{\Gamma}_{\alpha ij}(\omega) = 2\pi\sum_{\boldsymbol{k}\in\alpha} V^*_{i\alpha\boldsymbol{k}}V_{j\alpha\boldsymbol{k}}\delta(\omega - \epsilon_{\alpha\boldsymbol{k}})$ summarizes all the non-Markovian memory effects of the electron reservoirs on the dot system.

The correlation Green's function $\boldsymbol{v}(t)$ [Eq. (7b)] has a general solution in terms of the retarded Green's function $\boldsymbol{u}(\tau)$,

$$\boldsymbol{v}(\tau) = \int_{t_0}^{\tau} d\tau_1 \int_{t_0}^{t} d\tau_2 \boldsymbol{u}(\tau-\tau_1+t_0)\widetilde{\boldsymbol{g}}(\tau_1-\tau_2)\bar{\boldsymbol{u}}(\tau_2). \tag{9}$$

From the master equation [Eq. (4a)] it is easy to find the single-particle reduced density matrix in terms of $\boldsymbol{u}(t)$ and $\boldsymbol{v}(t)$,

$$\rho^{(1)}_{ij}(t) \equiv \mathrm{tr}[a^\dagger_j a_i \rho(t)] = u_{ii'}(t)\rho^{(1)}_{i'j'}(t_0)u^\dagger_{j'j}(t) + v_{ij}(t), \tag{10}$$

where $\rho^{(1)}_{ij}(t_0)$ is the initial single-particle reduced density matrix of the dots. The currents Eq. (4b) can then be explicitly expressed as[26]

$$I_{i\alpha}(t) = -2e\mathrm{Re}\int_{t_0}^{t} d\tau\{\boldsymbol{g}_\alpha(t-\tau)\boldsymbol{v}(\tau) - \widetilde{\boldsymbol{g}}_\alpha(t-\tau)\bar{\boldsymbol{u}}(\tau) + \boldsymbol{g}_\alpha(t-\tau)\boldsymbol{u}(\tau)\boldsymbol{\rho}^{(1)}(t_0)\bar{\boldsymbol{u}}^\dagger(t)\}_{ii}. \tag{11}$$

This expression is consistent with the result obtained from the Keldysh Green's function technique, except that the initial state dependence [the third term in Eq. (10)] is usually ignored in most of the Green's function treatments[28] (see the explicit derivation given in Ref. [26]). If the dot system is initially empty, namely, $\rho^{(1)}_{ij}(t_0) = 0$, the transient electronic occupations and currents can be further simplified:

$$\rho^{(1)}_{ij}(t) = v_{ij}(t), \tag{12a}$$

$$I_{i\alpha}(t) = -2e\mathrm{Re}\int_{t_0}^{t} d\tau\{\boldsymbol{g}_\alpha(t-\tau)\boldsymbol{v}(\tau) - \widetilde{\boldsymbol{g}}_\alpha(t-\tau)\bar{\boldsymbol{u}}(\tau)\}_{ii}. \tag{12b}$$

Thus, solving Eq. (7a) and using Eq. (9), we can obtain the full information of the transient quantum transport dynamics.

To be specific, we consider in this paper a double-quantum-dot AB interferometer schematically plotted in Fig. 1, where each of the quantum dots has a single active electronic state. Then the energy matrix $\boldsymbol{E}$ in Eq. (7) becomes a 2×2 matrix. We also do not consider the interdot tunnel coupling, namely, $E_{12} = E_{21} = 0$. The AB magnetic flux is embedded in the tunneling amplitudes between the leads and the dots: $V_{jL\boldsymbol{k}} = \bar{V}_{jL\boldsymbol{k}}e^{-i\phi_{jL}}$ and $V_{jR\boldsymbol{k}} = \bar{V}_{jR\boldsymbol{k}}e^{i\phi_{jR}}$ with the relation $\phi_{1L} - \phi_{2L} + \phi_{1R} - \phi_{2R} = \phi \equiv 2\pi\Phi/\Phi_0$, and $\Phi_0 = hc/e$ is the flux quantum. Thus, the spectral density involving explicitly the threading magnetic flux is given by

$$\boldsymbol{\Gamma}_{\alpha ij}(\omega) = 2\pi\sum_{\boldsymbol{k}\in\alpha}\bar{V}_{i\alpha\boldsymbol{k}}\bar{V}_{j\alpha\boldsymbol{k}}e^{\pm i(\phi_{i\alpha}-\phi_{j\alpha})}\delta(\omega-\epsilon_{\alpha\boldsymbol{k}}), \tag{13}$$

where the $+(-)$ sign is for $\alpha = L(R)$. With the above basic formulation, we are able to explore the nonequilibrium electronic dynamics in this nanoscale AB interferometer.

III. ANALYTICAL SOLUTIONS

We exploit in our calculations the ubiquitously used wide-band approximation, in which the spectral density is assumed to be frequency independent. In general, the magnetic phase can be characterized by two variables, the magnetic flux threading the ring, $\phi = \phi_L + \phi_R$, and the difference, that is, the gauge degree of freedom, $\chi = \frac{\phi_L - \phi_R}{2}$, where $\phi_\alpha = \phi_{1\alpha} - \phi_{2\alpha}$. Correspondingly, the spectral density is reduced to $\boldsymbol{\Gamma}_\alpha = \Gamma_\alpha\begin{pmatrix}1 & e^{\pm i\phi_\alpha}\\ e^{\mp i\phi_\alpha} & 1\end{pmatrix}$, where the upper (lower) sign is for $\alpha = L(R)$. The time-dependent self-energy correction to the retarded Green's function of the electron in the double dot is given by

$$\boldsymbol{g}(\tau) = \delta(\tau)\begin{pmatrix}\Gamma & e^{i\chi}\Gamma^+_\phi\\ e^{-i\chi}\Gamma^-_\phi & \Gamma\end{pmatrix}, \tag{14}$$

with $\Gamma^\pm_\phi = [\Gamma\cos(\phi/2) \pm i\delta\Gamma\sin(\phi/2)]$. Here $\Gamma = \Gamma_L + \Gamma_R$ and $\delta\Gamma = \Gamma_L - \Gamma_R$ characterize the strength and the asymmetry of the coupling to the leads, respectively.

Even for the most general case of a nondegenerate double dot asymmetrically coupled to the leads, the solution of Eq. (7a) can be found analytically (taking $t_0 = 0$):

$$\boldsymbol{u}(\tau) = u_0(\tau)\sigma_0 - u_p(\tau)\hat{\vec{p}}(\phi,\chi)\cdot\vec{\sigma}. \tag{15}$$

Here $\vec{\sigma} = (\sigma_+,\sigma_-,\sigma_z)$ is the vector of the three Pauli matrices, and $\sigma_0 = I$ (the identity operator). We have introduced a flux-dependent and gauge-dependent polarization vector $\vec{p}(\phi,\chi) \equiv (p_-(\phi,\chi),p_+(\phi,\chi),p_z(\phi,\chi)) = (\frac{1}{2}e^{i\chi}\Gamma_\phi^+,\frac{1}{2}e^{-i\chi}\Gamma_\phi^-,i\delta E)$ containing all the information on the gauge dependence, the flux dependence, and the dependence on the asymmetry of the couplings, with $\delta E = E_1 - E_2$ characterizing the nondegeneracy of the double-dot on-site energies. Here $\hat{\vec{p}}(\phi,\chi) = \vec{p}(\phi,\chi)/\Gamma_\phi$ and $\Gamma_\phi = \sqrt{\Gamma^2\cos^2(\phi/2) + \delta\Gamma^2\sin^2(\phi/2) - \delta E^2}$, which is gauge independent. Without loss of generality, we set $E = \frac{E_1+E_2}{2} = 0$ as an energy reference. Then the functions $u_0(\tau)$ and $u_p(\tau)$ in Eq. (15) are given by

$$u_{0,p}(\tau) = \tfrac{1}{2}\left[e^{-\gamma_\phi^-\tau} \pm e^{-\gamma_\phi^+\tau}\right], \tag{16}$$

with $\gamma_\phi^\pm = \frac{1}{2}(\Gamma \pm \Gamma_\phi)$, which are also gauge independent. Substituting Eq. (15) into Eq. (9), we obtain the correlation Green's function

$$\boldsymbol{v}(t) = \int \frac{d\omega}{2\pi}\boldsymbol{u}(t,\omega)\sum_\alpha f_\alpha(\omega)\boldsymbol{\Gamma}_\alpha\boldsymbol{u}^\dagger(t,\omega), \tag{17}$$

where $\boldsymbol{u}(t,\omega) = u_0(t,\omega)\sigma_0 - u_p(t,\omega)\hat{\vec{p}}(\phi,\chi)\cdot\vec{\sigma}$ and

$$u_{0,p}(t,\omega) = \frac{1}{2}\left[\frac{e^{(i\omega-\gamma_\phi^-)t}-1}{i\omega-\gamma_\phi^-} \pm \frac{e^{(i\omega+\gamma_\phi^+)t}-1}{i\omega-\gamma_\phi^+}\right]. \tag{18}$$

The gauge degree of freedom parametrized by χ appears explicitly in the off-diagonal matrix elements of the retarded and the correlation Green's functions $\boldsymbol{u}(t)$ and $\boldsymbol{v}(t)$. However, the physical observables, calculated from $\boldsymbol{u}(t)$ and $\boldsymbol{v}(t)$, do not depend on χ, ensuring the gauge invariance of our calculations.

Explicitly, the electronic occupation on each dot is given by the diagonal matrix element of $\boldsymbol{v}(t)$ [see Eq. (12a)]. The total occupation number $N(t) = n_1(t) + n_2(t)$, where $n_i(t) = v_{ii}(t)$, can be expressed explicitly as

$$\begin{aligned}N(t) = {}& \int \frac{d\omega}{2\pi}f_+(\omega)\left\{\Gamma\left[|u_0(t,\omega)|^2 + \left(\Gamma_\phi^2 + 2\delta E^2\right)\left|\frac{u_p(t,\omega)}{\Gamma_\phi}\right|^2\right] - 2\left(\Gamma_\phi^2+\delta E^2\right)\mathrm{Re}\left[\frac{u_0^*(t,\omega)u_p(t,\omega)}{\Gamma_\phi}\right]\right\}\\ &+ \int \frac{d\omega}{2\pi}f_-(\omega)\delta\Gamma\left\{|u_0(t,\omega)|^2 + \left(\Gamma_\phi^2 + 2\delta E^2 - (\Gamma^2-\delta\Gamma^2)\frac{\delta E}{\delta\Gamma}\sin\phi\right)\left|\frac{u_p(t,\omega)}{\Gamma_\phi}\right|^2 - 2\Gamma\mathrm{Re}\left[\frac{u_0^*(t,\omega)u_p(t,\omega)}{\Gamma_\phi}\right]\right\},\end{aligned} \tag{19}$$

and the occupation difference between the two dots, $\delta n(t) = n_1(t) - n_2(t)$, is given by

$$\delta n(t) = \int \frac{d\omega}{2\pi}\mathrm{Im}\left[u_0^*(t,\omega)\frac{u_p(t,\omega)}{\Gamma_\phi}\right]\left\{\Gamma\delta E f_+(\omega)\left[\delta\Gamma\delta E - \frac{\sin\phi}{2}(\Gamma^2-\delta\Gamma^2)\right]f_-(\omega)\right\}. \tag{20}$$

Here $f_\pm(\omega) \equiv f_L(\omega) \pm f_R(\omega)$.

On the other hand, the current passing from the left lead to the right one through dot i is given by $I_i = I_{Li} - I_{Ri}$. Summing up the two currents through the two dots, we obtain the transport net current $I = \frac{1}{2}(I_L - I_R)$. Combining the current I_1 flowing from the left to the right through the first dot with the current $-I_2$ flowing from the right to the left through the second dot gives the circulating current $I_c = I_1 - I_2$. Explicitly, the transient net current is given by

$$\begin{aligned}I(t) = {}& \int \frac{d\omega}{2\pi}f_+(\omega)\left\{\delta\Gamma\mathrm{Re}\left(u_0(t,\omega) - \frac{\Gamma}{\Gamma_\phi}u_p(t,\omega)\right) - \frac{\Gamma\delta\Gamma}{2}\left[2|u_0(t,\omega)|^2 + \left(\Gamma^2\left[\cos^2\frac{\phi}{2}\cos\phi + \frac{\sin^2\phi}{2} + \frac{\delta E}{\delta\Gamma}\sin\phi\right]\right.\right.\right.\\ &\left.\left.\left. - \delta\Gamma^2\left[\sin^2\frac{\phi}{2}\cos\phi - \frac{\sin^2\phi}{2} + \frac{\delta E}{\delta\Gamma}\sin\phi\right] + \Gamma_\phi^2 + \delta E^2\right)\left|\frac{u_p(t,\omega)}{\Gamma_\phi}\right|^2\right]\right.\\ &\left. + \left(\Gamma^2\delta\Gamma\left(\cos^2\frac{\phi}{2}+1\right) + \delta\Gamma^3\sin^2\frac{\phi}{2} + \frac{\Gamma^2-\delta\Gamma^2}{2}\delta E\sin\phi\right)\mathrm{Re}\left[\frac{u_0^*(t,\omega)u_p(t,\omega)}{\Gamma_\phi}\right]\right\}\\ &+ \int \frac{d\omega}{2\pi}f_-(\omega)\left\{\mathrm{Re}\left(\Gamma u_0(t,\omega) - \frac{\Gamma_\phi^2+\delta E^2}{\Gamma_\phi}u_p(t,\omega)\right) - \frac{\delta\Gamma^2\left(\cos^2\frac{\phi}{2}+1\right) + \Gamma^2\sin^2\frac{\phi}{2}}{2}|u_0(t,\omega)|^2\right.\\ &- \frac{1}{2}\left(\left[\Gamma^2\cos^2\frac{\phi}{2} - \delta\Gamma^2\sin^2\frac{\phi}{2} - \delta E^2\right]\delta\Gamma^2\cos^2\frac{\phi}{2} - \left[\Gamma^2\cos^2\frac{\phi}{2} - \delta\Gamma^2\sin^2\frac{\phi}{2} + \delta E^2\right]\Gamma^2\sin^2\frac{\phi}{2}\right.\\ &\left.\left.\left. + \delta\Gamma^2\left(\Gamma_\phi^2 + \Gamma^2\sin^2\phi + 2\delta E^2\right)\right)\left|\frac{u_p(t,\omega)}{\Gamma_\phi}\right|^2 + 2\Gamma\delta\Gamma^2\mathrm{Re}\left[\frac{u_0^*(t,\omega)u_p(t,\omega)}{\Gamma_\phi}\right]\right\},\end{aligned} \tag{21}$$

where the dependencies on χ in the Green's functions $\boldsymbol{u}$ and $\boldsymbol{v}$ are exactly canceled by those of the self-energy corrections $\tilde{\boldsymbol{g}}$ and $\boldsymbol{g}$ [see Eq. (12b)], leaving the current gauge independent. The transient circulating current is given by

$$I_c(t) = \int \frac{d\omega}{2\pi} f_+(\omega)\mathrm{Im}\Bigg\{ -\frac{u_p(t,\omega)}{\Gamma_\phi}(\Gamma^2 - \delta\Gamma^2)\sin\phi + \delta\Gamma\delta E\left[2\frac{u_p(t,\omega)}{\Gamma_\phi} - \Gamma u_0^*(t,\omega)\frac{u_p(t,\omega)}{\Gamma_\phi}\right]\Bigg\} + \int \frac{d\omega}{2\pi} f_-(\omega)\mathrm{Im}\Bigg\{ u_0^*(t,\omega)\frac{u_p(t,\omega)}{\Gamma_\phi}\frac{\delta\Gamma}{2}(\Gamma^2 - \delta\Gamma^2) \times \sin\phi + \delta E\left[2\Gamma\frac{u_p(t,\omega)}{\Gamma_\phi} - \delta\Gamma^2 u_0^*(t,\omega)\frac{u_p(t,\omega)}{\Gamma_\phi}\right]\Bigg\}. \tag{22}$$

These dynamical quantities depend on the amount of the nondegeneracy δE, the coupling asymmetry $\delta\Gamma$, the magnetic flux ϕ, and also the bias voltage applied on the leads through the particle distributions in the two electronic reservoirs. The time scales for the transient behaviors of these physical observables are determined by the factors $1/\gamma_\phi^\pm = 2/(\Gamma \pm \Gamma_\phi)$ in Eq. (16), in which the flux as well as the coupling asymmetry and the nondegeneracy play their important roles.

The symmetric and degenerate double-dot interferometer has been widely studied in the literature. This corresponds to $\delta E = \delta\Gamma = 0$. Thus, $\Gamma_\phi = \Gamma|\cos\frac{\phi}{2}|$, and the above results can be significantly simplified. Explicitly, the total occupation number in the double dot is reduced to

$$N(t) = \Gamma\int \frac{d\omega}{2\pi} f_+(\omega)\{|u_0(t,\omega)|^2 + |u_p(t,\omega)|^2 - 2|\cos(\phi/2)|\mathrm{Re}[u_0^*(t,\omega)u_p(t,\omega)]\}, \tag{23}$$

and the occupation difference between the two dots becomes

$$\delta n(t) = \Gamma\sin(\phi/2)\frac{\cos(\phi/2)}{|\cos(\phi/2)|} \times \int \frac{d\omega}{2\pi} f_-(\omega)\mathrm{Im}[u_0^*(t,\omega)u_p(t,\omega)]. \tag{24}$$

The transient net current is simplified to be

$$I(t) = \int \frac{d\omega}{2\pi} f_-(\omega)\Bigg\{ -\Gamma^2\frac{|u_0(t,\omega)|^2 - |u_p(t,\omega)|^2}{2}\sin^2\frac{\phi}{2} + \Gamma\mathrm{Re}[u_0(t,\omega) - |\cos(\phi/2)|u_p(t,\omega)]\Bigg\} \tag{25}$$

and the circular current is given by

$$I_c(t) = -\Gamma\sin(\phi/2)\frac{\cos(\phi/2)}{|\cos(\phi/2)|}\int \frac{d\omega}{2\pi} f_+(\omega)\mathrm{Im}[u_p(t,\omega)]. \tag{26}$$

In general, the transient flux dependence of the physical quantities [Eqs. (19)–(22)] for nondegenerate double dot with asymmetric couplings to the leads is neither symmetric nor antisymmetric in the flux. The complicated flux dependencies are mainly determined by the energy splitting δE. When the two quantum dots are set at degeneracy, $\delta E = 0$, regardless of the coupling asymmetry and the finite applied bias, both the total occupation number and the net current become symmetric in the flux, namely, $N(\phi,t) = N(-\phi,t)$ and $I(\phi,t) = I(-\phi,t)$. In contrast, the occupation difference and the circulating current become antisymmetric in the flux: $\delta n(\phi,t) = -\delta n(-\phi,t)$ and $I_c(\phi,t) = -I_c(-\phi,t)$. However, when the degeneracy is lifted, both the symmetric and antisymmetric flux dependencies are transiently present in all these physical observables. These complicated flux dependencies can be simplified by setting an applied bias, $\mu_L = \mathrm{eV}/2 = -\mu_R$. Under such a bias configuration, the terms involving $f_-(\omega)$ in Eqs. (20) and (22) vanish since both $\mathrm{Im}[u_0^*(t,\omega)u_p(t,\omega)]$ and $\mathrm{Im}[u_p(t,\omega)]$ are odd in ω while $f_-(\omega)$ is even in ω. The difference in the occupations of the two dots then becomes symmetric in the flux, $\delta n(\phi,t) = \delta n(-\phi,t)$, and is proportional to δE. On the other hand, the circulating current generally contains two contributions. One is proportional to $(\Gamma^2 - \delta\Gamma^2)\sin(\phi)$ and is antisymmetric in the flux. The other contribution is proportional to $\delta\Gamma\delta E$, and is symmetric in the flux. However, we find that the second contribution decays to zero within a time scale of a few $1/\Gamma$. After that time, the circulating current becomes antisymmetric in the flux, proportional to $\sin(\phi)$. Applying the aforementioned bias configuration does not affect the existence of both the symmetric and the antisymmetric flux-dependent components of the total occupation and the transient net current. Only in the special case of zero bias does the total occupation number become symmetric in the flux. The transient net current always has a nonvanishing antisymmetric flux dependence for arbitrary values of the bias when $\delta E \neq 0$.

More interestingly, during the transient transport processes, $I(\phi,t) \neq I(-\phi,t)$ for the nondegenerate case. In other words, it transiently breaks the well-known phase rigidity at arbitrary biases. This is easily understood because during the nonequilibrium transient processes there is no time-reversal symmetry. The time-reversal symmetry is the prerequisite for phase rigidity of the linear conductance of a two-terminal device.[4,6,7] Only at steady state, as we show in the next section, can Eq. (21) reproduce this phase rigidity, independent of the value of δE. The on-site energy splitting thus plays a crucial role for the time-reversal symmetry breaking with respect to the flux dependency during the transient dynamics. Note also that $I(\phi,t) \neq I(-\phi,t)$ is a purely transient effect. In a steady state, the phase rigidity is preserved.

IV. COHERENCE AND PHASE RIGIDITY AT STEADY STATE

Before studying the real-time dynamics of electronic transport in the double-dot AB interferometer, we deduce the steady-state results from the general formalism outlined in Sec. III, and compare them with the previously obtained ones.

The electronic occupation and the currents at steady state are obtained from Eqs. (19)–(22), upon using there $\lim_{t\to\infty} u_{0,p}(t,\omega) = [u_-(\omega) \pm u_+(\omega)]/2$, where $u_\pm(\omega) = 1/(\gamma_\phi^\pm - i\omega)$. Then, the total electronic

occupation is

$$N(\phi)=\Gamma\int_{-\infty}^{\infty}\frac{d\omega}{2\pi}f_+(\omega)\frac{(\omega^2+\gamma_\phi^+\gamma_\phi^-)}{[\omega^2+(\gamma_\phi^+)^2][\omega^2+(\gamma_\phi^-)^2]}+\int_{-\infty}^{\infty}\frac{d\omega}{2\pi}f_-(\omega)\left\{\frac{\delta\Gamma(\omega^2-\gamma_\phi^+\gamma_\phi^-)}{[\omega^2+(\gamma_\phi^+)^2][\omega^2+(\gamma_\phi^-)^2]}+\delta E\frac{\frac{\delta\Gamma\delta E}{2}-\frac{\Gamma^2-\delta\Gamma^2}{4}\sin(\phi)}{[\omega^2+(\gamma_\phi^+)^2][\omega^2+(\gamma_\phi^-)^2]}\right\}. \quad (27)$$

At zero bias, only the first term survives, while at finite bias the difference of the particle distributions between the two electronic reservoirs may give an additional contribution. This happens provided that the on-site energies of the two dots and their respective coupling to the leads are different. Remarkably, under these circumstances the total occupation includes also a component antisymmetric in the flux. In a rather similar fashion, the occupation difference between the two dots,

$$\delta n(\phi)=\int_{-\infty}^{\infty}\frac{\omega d\omega}{2\pi}\times\frac{\Gamma\delta E f_+(\omega)+\left(\delta\Gamma\delta E-\frac{(\Gamma^2-\delta\Gamma^2)}{2}\sin(\phi)\right)f_-(\omega)}{(\omega^2+(\gamma_\phi^+)^2)(\omega^2+(\gamma_\phi^-)^2)}, \quad (28)$$

is nonzero provided that the two dots are not degenerate, or when the bias is finite.

The steady-state net current takes the ubiquitous form

$$I(\phi)=\int\frac{d\omega}{2\pi}[f_L(\omega)-f_R(\omega)]\mathcal{T}(\omega,\phi), \quad (29)$$

with the transmission coefficient

$$\mathcal{T}(\omega,\phi)=\frac{(\Gamma^2-\delta\Gamma^2)\left[\omega^2\cos^2\frac{\phi}{2}+\left(\frac{\delta E}{2}\sin\frac{\phi}{2}\right)^2\right]}{[\omega^2+(\gamma_\phi^+)^2][\omega^2+(\gamma_\phi^-)^2]}. \quad (30)$$

This current (as well as its derivative with respect to the bias, that is, the differential conductance) obeys phase rigidity $I(\phi)=I(-\phi)$.[29] The expression for the transmission [Eq. (30)] reproduces the result of Ref. 14 when $\delta\Gamma=0$; further assuming that $\delta E=0$ yields the result quoted in Ref. 15.

Finally, the steady-state circulating current is

$$I_c(\phi)=(\Gamma^2-\delta\Gamma^2)\int_{-\infty}^{\infty}\frac{\omega d\omega}{2\pi}\times\frac{-\frac{\Gamma}{2}\sin(\phi)f_+(\omega)+\left(\delta E+\frac{\delta\Gamma}{2}\sin(\phi)\right)f_-(\omega)}{[\omega^2+(\gamma_\phi^+)^2][\omega^2+(\gamma_\phi^-)^2]}. \quad (31)$$

As expected, the circulating current is nonzero at zero bias and is proportional to $\sin(\phi)$. The oscillation amplitude of both the net and the circulating currents is determined by $\Gamma^2-\delta\Gamma^2$ and hence decreases as the coupling asymmetry is increased. When $\delta\Gamma=\Gamma$, the double dot is coupled to a single lead. The net current then vanishes, and so does the circulating current, because in our setup the ring is then "open" (see Fig. 1).

It is worth noting that for a degenerate double dot at zero flux, the operator $A_-^\dagger A_-$, where $A_-=(e^{-i\chi/2}a_1-e^{i\chi/2}a_2)/\sqrt{2}$ and χ is the gauge degree of freedom, gives a constant of motion:[31] $[A_-^\dagger A_-,\mathcal{H}]=0$. When one turns on a finite flux, this symmetry is broken, and the electronic occupation is changed significantly from its zero-flux value. Indeed, setting $\delta E=0$ and $\phi=0$ in Eq. (15) and taking the steady-state limit yields $N(\phi=0)=1/2+(\delta\Gamma/\pi\Gamma)\tan^{-1}(\mathrm{eV}/2\Gamma)$ at zero temperature. However, when one first takes the steady-state limit and only then the zero-flux one, the result is different, being $N(\phi\to0)=1-(\delta\Gamma/(2\Gamma)+(\delta\Gamma/\pi\Gamma)\tan^{-1}(\mathrm{eV}/2\Gamma)$ at zero temperature. Hence, $N(\phi=0)\neq N(\phi\to0)$, namely the total occupation changes abruptly across the zero-flux point. On the other hand, Eq. (20) yields that at degeneracy $\delta n(\phi=0,t)=\lim_{\phi\to0}\delta n(\phi,t)=0$, namely the occupation difference δn is continuous across the zero-flux point. By setting first $\delta E=0$ and $\phi=0$ in Eq. (15) and then taking the steady-state limit, compared with the limit $\phi\to0$ after the steady-state limit is taken, we find that both I and I_c are continuous as the zero-flux point is crossed. Thus, the abrupt change upon crossing zero flux occurs only in the total electronic occupation due to the existence of an occupation constant of motion at $\phi=0$.

V. REAL-TIME DYNAMICS

Having obtained analytical solutions for the electronic occupations and the transport currents in the double-dot AB interferometer for an initial empty state, we now examine the way these quantities approach the steady state, namely, their real-time dynamics. For simplicity, we exploit below the bias configuration $\mu_L=\mathrm{eV}/2=-\mu_R$.

A. Degenerate double dot with asymmetric couplings to the leads ($\delta E=0$, $\delta\Gamma\neq0$)

At degeneracy, electron transport through the double dot is mediated via the two orthogonal states, $A_\pm^\dagger|0\rangle=[(e^{-i\chi/2}a_1\pm e^{i\chi/2}a_2)/\sqrt{2}]|0\rangle$, associated with the decay rates $\gamma_\phi^\pm$. When $\phi=0$, the state $A_-^\dagger|0\rangle$ is decoupled from the leads, and transport is accomplished only through $A_+^\dagger|0\rangle$. The transient process is governed by the corresponding decay rate $\gamma_{\phi=0}^+=(\Gamma+\Gamma_{\phi=0})/2=\Gamma$. Once a finite flux is applied, the state $A_-^\dagger|0\rangle$ also participates in the transport. The rate γ_ϕ^- associated with this state is very small, $\gamma_\phi^-\sim\Gamma\phi^2$, when ϕ deviates slightly from zero and consequently the time required to reach the steady state at small fluxes is much longer than that for $\phi=0$. The nonequilibrium occupation dynamics of the system with and without a threading magnetic flux becomes therefore significantly different. This is in particular manifested by the temporal evolution of the occupations, shown in Fig. 2(a), where it is seen that the curve for $t=40/\Gamma$ deviates considerably from the curve for $t=\infty$ for fluxes near zero and that the occupation at $t\to\infty$ is discontinuous. On the other hand, both the net and the circulating currents are continuous across the zero-flux point, and therefore the long times needed for the occupation to reach steady-state near zero flux are not expected for these currents, as indeed is exemplified in Figs. 2(b) and 2(c).

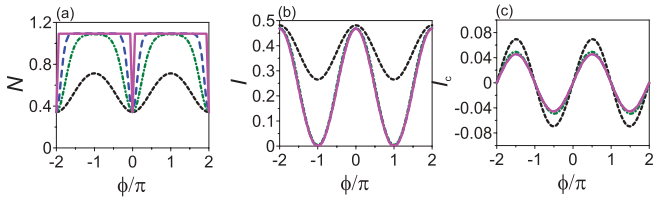

FIG. 2. (Color online) Flux dependence of the occupations and currents at several different times for $\delta E = 0$. The quantum dots are initially empty. The difference in the occupation numbers is not shown since it remains zero at degeneracy. The black short-dashed line is for $t = 2/\Gamma$, the green dash-dotted line is for $t = 10/\Gamma$, the blue long-dashed line is for $t = 40/\Gamma$, and $t = \infty$ is the magenta solid line. The bias is $eV = 3\Gamma$, the asymmetric coupling is $\delta\Gamma = -0.5\Gamma$, and the temperature is $k_BT = \Gamma/20$. The parameters used here are also used in other figures unless otherwise stated.

B. Nondegenerate double dot with symmetric coupling to the leads ($\delta E \neq 0, \delta\Gamma = 0$)

The effect of a finite on-site energy splitting, δE, on the temporal evolution is examined in Figs. 3. When this splitting is small, for example, $\delta E = 0.15\Gamma$, the times needed for the occupations to reach their steady-state values at fluxes near zero are much longer than those at other values of the flux [compare Figs. 3(a2) and 3(b2) at $t = 40/\Gamma$ with Figs. 3(a3) and 3(b3) at $t = \infty$]. Increasing further the splitting, for example $\delta E \sim \Gamma$, the decay rates $\gamma_\phi^\pm$ become less sensitive to the flux [see the curves for $\delta E > 0.5\Gamma$ in Figs. 3(a2) and 3(b2) and Figs. 3(a3) and 3(b3)].

The nondegeneracy also plays an important role in determining the flux-dependence profiles of the electron occupations. At short times, for example, $t = 2/\Gamma$ [see Figs. 3(a1) and 3(b1)], these are dominated by the symmetric flux dependence. As the time approaches tens of $1/\Gamma$, the antisymmetric-flux dependence becomes distinct [see Figs. 3(a2) and 3(b2) at $t = 40/\Gamma$]. Such antisymmetry in the flux reflects a preferred direction of the electron circulation, which is dictated by the on-site energy splitting, and hence is missing when the double dot is degenerate. Indeed, as can be seen from the last term on the right-hand side of Eq. (27), the antisymmetric term in the occupation disappears when $\delta E = 0$. Then, the line shape shows a plateaulike structure with a discontinuity, as explained in Sec. IV. The saw-tooth structures in Figs. 3(a2)–3(a3) and Figs. 3(b2)–3(b3) can be understood by examining Eqs. (A1b). The part of the occupation antisymmetric in the flux approaches $\cot(\phi/2)$ when $eV \gg \Gamma$, and $\cot(\phi/2)/\sin^2(\phi/2)$ when $eV \ll \Gamma$, provided that the energy splitting δE appearing in the denominators in Eqs. (27) is ignored. Therefore, at small energy splitting, the $\cot(\phi/2)$ will give rise to a sharp saw-tooth structure, which gradually disappears as the on-site energy splitting is increased.

Turning now to the net current, we observe that the line shapes corresponding to different δE's at time $t = 2/\Gamma$ shown in Fig. 3(c1), have a different phase shift as compared to those at later times, shown in Figs. 3(c2) and 3(c3). This exemplifies the breaking of phase rigidity in the transient net current,

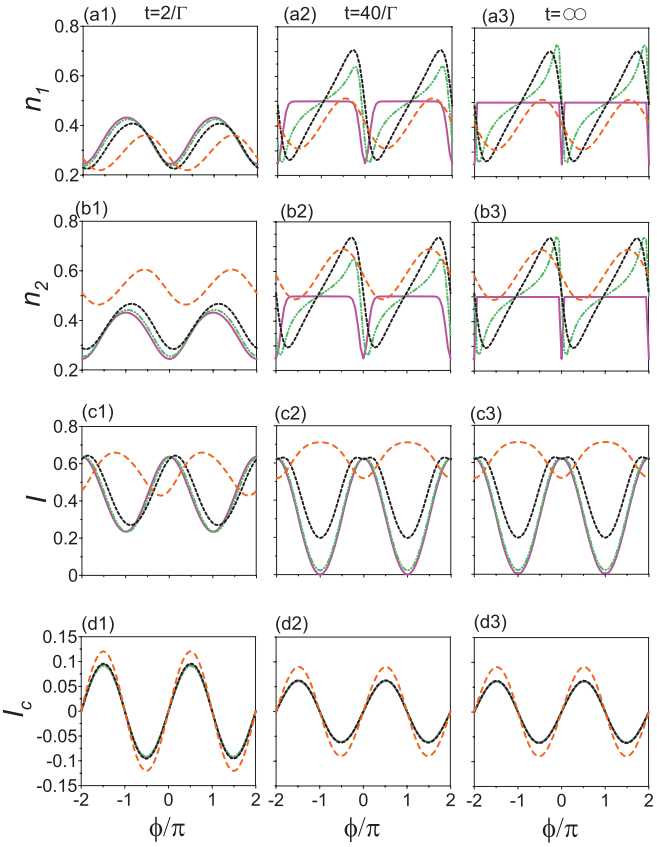

FIG. 3. (Color online) Flux dependencies of the occupations and currents at several different times with various energy splittings δE. The magenta solid lines are for $\delta E = 0$, the green lines are for $\delta E = 0.15\Gamma$, the black short-dashed lines are for $\delta E = 0.5\Gamma$, and the orange long-dashed lines are for $\delta E = 2\Gamma$.

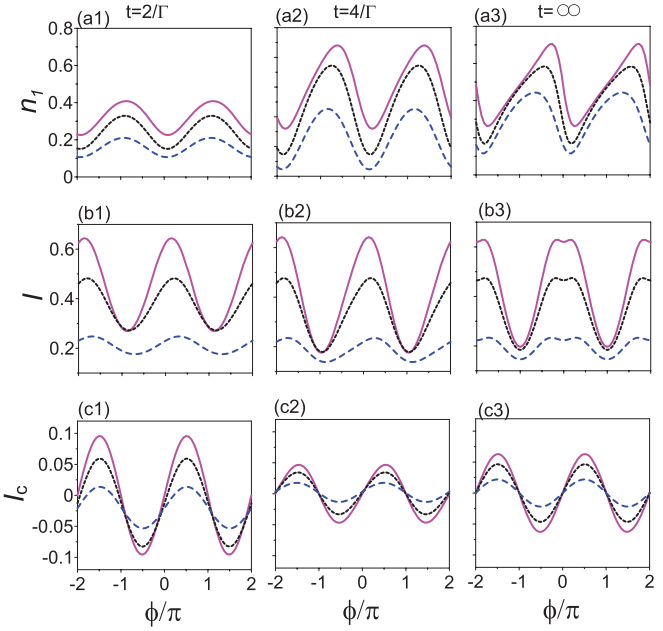

FIG. 4. (Color online) The occupation number of the first dot, the net current, and the circulating current as functions of flux in (a1) to (a3), (b1) to (b3), and (c1) to (c3), respectively, with $\delta E = 0.5\Gamma$. The magenta solid lines are for $\delta\Gamma = 0$, the black short-dashed lines are for $\delta\Gamma = -0.5\Gamma$ and the blue long-dashed lines are for $\delta\Gamma = -0.8\Gamma$.

as discussed in connection with Eq. (21). In contrast, phase rigidity remains at all times for a degenerate double dot (see Figs. 2). The circulating current, shown in Figs. 3(d1)–3(d3), is almost insensitive to changes in the on-site energy splitting, as expected from Eq. (22).

C. Nondegenerate double dot with asymmetric coupling to the leads ($\delta E \neq 0, \delta\Gamma \neq 0$)

We next study the combined effect of both the asymmetric coupling and a finite energy splitting.

Figures 4 depict the occupations and currents for various choices of $\delta\Gamma$'s with $\delta E = 0.5\Gamma$. The occupation of the second quantum dot is not shown for this energy splitting since n_2 does not differ much from n_1. At short times, for example, $t = 2/\Gamma$, the occupations corresponding to different asymmetries $\delta\Gamma$'s have identical AB oscillation phases [see Fig. 4(a1)] while at longer times, these tend to differ [Figs. 4(a2) and 4(a3)]. The amplitudes of both the transient net current and the circulating current decrease upon increasing the coupling asymmetry [see Figs. 4(b1)–4(c3)], as expected. Concomitantly, the antisymmetric-flux component of the occupations becomes less distinct [see Figs. 4(a1)–4(a3)]. Inspecting the curves in Fig. 4(c1), one sees that the flux dependence of the circulating current has a small deviation from the $\sin\phi$ profile during an initial short time, but then reaches the line shape proportional to $\sin\phi$.

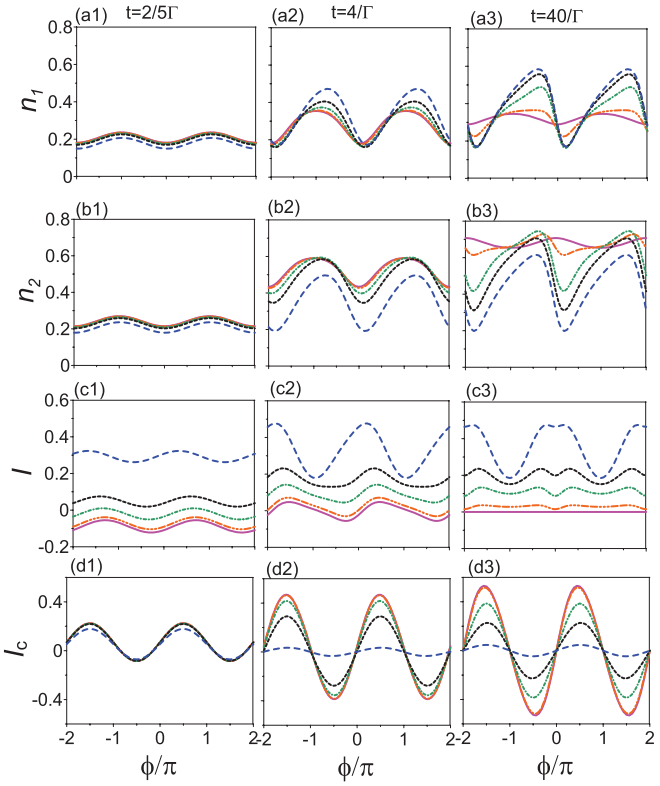

FIG. 5. (Color online) The occupation numbers (a1)–(b3), the net current (c1)–(c3), and the circulating current (d1)–(d3) as functions of flux. The magenta solid lines are for eV = 0, the orange dash-dash-dot-dot-dot lines are for eV = 0.0125Γ, the green dash-dot lines are for eV = 0.5Γ, the black short-dashed lines are for eV = Γ, and the blue long-dashed lines are for eV = 3Γ.

We next examine the effects of varying the bias voltage. The flux dependence profiles of the electronic occupations for various values of eV are plotted in Figs. 5(a1)–5(b3), for $\delta E = 0.5\Gamma$ and $\delta\Gamma = -0.5\Gamma$. At zero bias, the occupation numbers are symmetric in the flux at all times, just as at equilibrium [see Figs. 5(a1)–5(a3) and 5(b1)–5(b3)]. A finite bias modifies the line shapes of the individual occupations of the two dots, as can be seen by comparing Figs. 5(a2) and 5(a3) with Figs. 5(b2) and 5(b3). The symmetric flux dependence of the net current is transiently broken for all biases [see Figs. 5(c1) and 5(c2)], due to the nondegeneracy. At zero bias, the net current goes to zero at steady state, as expected, but a finite transient net current is observed [see the curve for eV = 0 in Figs. 5(c1) and 5(c2)]. The antisymmetric flux dependence is maintained for the circulating current, and only the AB oscillation amplitudes vary in time at different values of the bias [see Figs. 5(d1) and 5(d3)].

Finally, we note that the plateau line shapes depicted in Fig. 5(c) can be understood by exploiting the second of Eqs. (A3b). Differentiating that result with respect to ϕ yields

$$\frac{\partial I(\phi)}{\partial\phi} = (\Gamma^2 - \delta\Gamma^2)\sin(\phi) \times \left(\left[\frac{\Gamma^2 - \delta\Gamma^2}{\delta E^2}\sin^2(\phi/2) + 1\right]^{-1} - 1\right). \quad (32)$$

Hence, the bigger is the on-site energy splitting δE, the wider is the region in which the derivative is almost zero, leading to the appearance of the plateaus.

VI. CONCLUSIONS

In this work we have explored the transient quantum dynamics of a double-quantum-dot AB interferometer using the exact solution of the master equation. We analyzed the effects of various tunable parameters of the system, namely, the splitting of the on-site energies on the double dot, the asymmetric coupling to the left and the right leads, and the externally applied bias, on the time-dependent electronic occupations and the net current as well as on the circulating current, during the nonequilibrium transient processes. In the steady-state limit, we recover the results that have been extensively investigated in the literature.

With identical on-site energies on the double dot, regardless of the coupling asymmetry to the leads, we find that the total electronic occupation in the double dot and the net current are always symmetric in the flux, while the occupation difference between the two dots and the circulating current are antisymmetric in it. We also find that the time needed for the total occupation to reach its steady-state value is much longer near zero flux, compared with the flux values away from zero. This is because there exists an occupation symmetry at zero flux, where a discontinuity across zero flux in the total occupation is found. By breaking the degeneracy of the double dot, the phase rigidity in the net current is broken transiently at an arbitrary value of the bias. By varying the nondegeneracy of the double dot and the coupling asymmetry to the leads, the total occupation has an arbitrary flux dependence at finite biases. The nondegenerate double dot with an asymmetric

coupling to the leads makes the circulating current to slightly deviate from the antisymmetric flux dependence initially, but it then quickly approaches the AB oscillations with the fully antisymmetric flux dependence. It is also shown that a small bias causes a large circulating current, whereas the net current is negligible. Thus, measuring the circulating current may provide new insights into electron coherence during the transport.

In short, the splitting of the on-site energies on the double dot and the bias configuration applied to the leads change significantly the flux dependencies of the transient electronic occupations as well as the transient transport currents. We hope that experimentally monitoring the transient evolution will deepen our understanding of the electronic dynamics in quantum-dot AB interferometers.

ACKNOWLEDGMENTS

This work is partially supported by the National Science Council (NSC) of ROC under Contract No. NSC-99-2112-M-006-008-MY3. We also acknowledge support from the National Center for Theoretical Science of NSC and the High Performance Computing Facility in the National Cheng Kung University. OEW and AA acknowledge support from the Israel Science Foundation. JJ acknowledges support from the National Natural Science Foundation of China NSFC-10904029.

APPENDIX: SMALL AND LARGE BIAS LIMITS OF THE STEADY STATE AT ZERO TEMPERATURE

The steady-state occupation numbers and currents [Eqs. (27)–(31)] are expressed in terms of integrals over the frequency. These integrals can be explicitly carried out at zero temperature with the bias configuration $\mu_L = \mathrm{eV}/2 = -\mu_R$.

At zero temperature, the total electronic occupation is found to be

$$N(\phi) = 1 + \left(\delta\Gamma - \delta E \frac{\frac{\delta\Gamma\delta E}{2} - \frac{\Gamma^2-\delta\Gamma^2}{4}\sin\phi}{\Gamma\gamma_\phi^+}\right)\frac{\tan^{-1}\left[\frac{\mathrm{eV}/2}{\gamma_\phi^+}\right]}{\pi\Gamma_\phi} - \left(\delta\Gamma - \delta E \frac{\frac{\delta\Gamma\delta E}{2} - \frac{\Gamma^2-\delta\Gamma^2}{4}\sin\phi}{\Gamma\gamma_\phi^-}\right)\frac{\tan^{-1}\left[\frac{\mathrm{eV}/2}{\gamma_\phi^-}\right]}{\pi\Gamma_\phi}. \tag{A1a}$$

Assuming a small or a large bias, Eq. (A1) can be further simplified,

$$N(\phi) \to 1 + \begin{cases} \frac{\mathrm{eV}}{2\pi\gamma_\phi^+\gamma_\phi^-}\left[\delta E \frac{2\delta\Gamma\delta E - (\Gamma^2-\delta\Gamma^2)\sin\phi}{4\gamma_\phi^+\gamma_\phi^-} - \delta\Gamma\right] & \text{if } \mathrm{eV} \ll \Gamma, \\ \frac{\delta E}{2\Gamma}\frac{2\delta E\delta\Gamma - (\Gamma^2-\delta\Gamma^2)\sin\phi}{(\Gamma^2-\delta\Gamma^2)\sin^2(\phi/2)+\delta E^2} & \text{if } \mathrm{eV} \gg \Gamma. \end{cases} \tag{A1b}$$

Note that since Coulomb interactions have been ignored, the screening effect is altogether discarded. By setting $\delta E = 0$, the total occupation at large bias becomes independent of the flux. In contrast, at small bias the total occupation is flux dependent when the coupling to the leads becomes asymmetric.

The occupation difference between the two dots at zero temperature reads

$$\delta n(\phi) = \begin{cases} \frac{\delta E}{2\pi\Gamma_\phi}\ln\frac{(\mathrm{eV}/2)^2+(\gamma_\phi^-)^2}{(\mathrm{eV}/2)^2+(\gamma_\phi^+)^2} & \text{if } \Gamma_\phi \text{ is real}, \\ \frac{\delta E}{\pi|\Gamma_\phi|}\left[\tan^{-1}\frac{(\mathrm{eV})^2+\Gamma^2-|\Gamma_\phi|^2}{2\Gamma|\Gamma_\phi|^2} - \frac{\pi}{2}\right] & \text{otherwise}. \end{cases} \tag{A2a}$$

As expected, the occupation difference is proportional to δE. The small and large bias limits are

$$\delta n(\phi) \to \begin{cases} \frac{\delta E}{\pi\Gamma_\phi}\ln\frac{\gamma_\phi^-}{\gamma_\phi^+} & \text{if } \mathrm{eV} \ll \Gamma, \\ 0 & \text{if } \mathrm{eV} \gg \Gamma, \end{cases} \tag{A2b}$$

when Γ_ϕ is real, and otherwise

$$\delta n(\phi) \to \begin{cases} \frac{\delta E}{\pi|\Gamma_\phi|}\left[\tan^{-1}\frac{\Gamma^2-|\Gamma_\phi|^2}{2\Gamma|\Gamma_\phi|^2} - \frac{\pi}{2}\right] & \text{if } \mathrm{eV} \ll \Gamma, \\ 0 & \text{if } \mathrm{eV} \gg \Gamma. \end{cases} \tag{A2c}$$

Therefore, when a small bias is applied, the on-site energy splitting effectively causes a difference in the occupations. However, when we apply a bias much larger than the energy splitting, the energy splitting becomes ineffective in rendering the occupation difference between the two dots. The bias setting with respect to the energy splitting is thus essential for the control of the occupation difference between the two dots.

Having examined the occupations in these limits, we now turn to the currents. The steady-state net current at zero temperature is found to be

$$I(\phi) = \frac{(\Gamma^2-\delta\Gamma^2)}{\pi\Gamma\Gamma_\phi}\left\{\left(\gamma_\phi^+\cos^2\frac{\phi}{2} - \frac{\delta E^2\sin^2\frac{\phi}{2}}{4\gamma_\phi^+}\right)\times\tan^{-1}\left[\frac{\mathrm{eV}/2}{\gamma_\phi^+}\right] - \left(\gamma_\phi^-\cos^2\frac{\phi}{2} - \frac{\delta E^2\sin^2\frac{\phi}{2}}{4\gamma_\phi^-}\right)\times\tan^{-1}\left[\frac{\mathrm{eV}/2}{\gamma_\phi^-}\right]\right\}. \tag{A3a}$$

For small or large biases, it is further reduced to

$$I(\phi) \to (\Gamma^2-\delta\Gamma^2) \times \begin{cases} \frac{\mathrm{eV}}{8\pi(\gamma_\phi^+\gamma_\phi^-)^2}\delta E^2\sin^2\frac{\phi}{2} & \text{if } \mathrm{eV} \ll \Gamma, \\ \frac{1}{2\Gamma}\left[\cos^2\frac{\phi}{2} + \frac{\delta E^2\sin^2\frac{\phi}{2}}{(\Gamma^2-\delta\Gamma^2)\sin^2\frac{\phi}{2}+\delta E^2}\right] & \text{if } \mathrm{eV} \gg \Gamma. \end{cases} \tag{A3b}$$

In the small bias limit, the amplitude of the AB oscillation in the net current increases with the on-site energy splitting. However, under a large bias, it shows two competing oscillations, $\cos^2(\phi/2)$ and $\sin^2(\phi/2)$, where higher harmonics are accompanied with the energy splitting δE.

The explicit expression for the steady-state circulating current at zero temperature is

$$I_c(\phi) = -\frac{\Gamma^2-\delta\Gamma^2}{2\pi}\sin\phi \times \begin{cases} \frac{1}{2\Gamma_\phi}\ln\frac{(eV/2)^2+(\gamma_\phi^-)^2}{(eV/2)^2+(\gamma_\phi^+)^2} & \text{if } \Gamma_\phi \text{ is real,} \\ \frac{1}{|\Gamma_\phi|}\left[\tan^{-1}\frac{(eV)^2+\Gamma^2-|\Gamma_\phi|^2}{2\Gamma|\Gamma_\phi|^2}-\frac{\pi}{2}\right] & \text{otherwise,} \end{cases} \tag{A4a}$$

and for small or large biases it reads

$$I_c(\phi) \to \begin{cases} -\frac{(\Gamma^2-\delta\Gamma^2)}{2\pi\Gamma_\phi}\sin\phi\ln\frac{\gamma_\phi^-}{\gamma_\phi^+} & \text{if } eV \ll \Gamma, \\ 0 & \text{if } eV \gg \Gamma, \end{cases} \tag{A4b}$$

when Γ_ϕ is real, and otherwise

$$I_c(\phi) \to \begin{cases} -\frac{(\Gamma^2-\delta\Gamma^2)}{2\pi|\Gamma_\phi|}\sin\phi\left[\tan^{-1}\frac{\Gamma^2-|\Gamma_\phi|^2}{2\Gamma|\Gamma_\phi|^2}-\frac{\pi}{2}\right] & \text{if } eV \ll \Gamma, \\ 0 & \text{if } eV \gg \Gamma. \end{cases} \tag{A4c}$$

From the above results we find that the circulating current becomes significantly large when the bias is sufficiently small. In the opposite limit, the large bias drives the electron to flow in one direction and the circulating motion is then strongly suppressed.

*wzhang@mail.ncku.edu.tw
†orawohlman@bgu.ac.il; also at Tel Aviv University, Tel Aviv 69978, Israel.
‡aaharonyaa@bgu.ac.il; also at Tel Aviv University, Tel Aviv 69978, Israel.

[1] M. Büttiker, Phys. Rev. B **46**, 12485 (1992).
[2] Y. Imry, *Introduction to Mesoscopic Physics*, 2nd ed. (Oxford University Press, Oxford, 2002).
[3] I. L. Aleiner, Ned S. Wingreen, and Y. Meir, Phys. Rev. Lett. **79**, 3740 (1997).
[4] A. Yacoby, M. Heiblum, D. Mahalu, and H. Shtrikman, Phys. Rev. Lett. **74**, 4047 (1995).
[5] R. Schuster, E. Buks, M. Heiblum, D. Mahalu, V. Umansky, and H. Shtrikman, Nature (London) **385**, 417 (1997).
[6] A. Yacoby, R. Schuster, and M. Heiblum, Phys. Rev. B **53**, 9583 (1996).
[7] A. Levy Yeyati and M. Büttiker, Phys. Rev. B **52**, 14360R (1995).
[8] G. Hackenbroich and H. A. Weidenmüller, Phys. Rev. Lett. **76**, 110 (1996).
[9] C. Bruder, R. Fazio, and H. Schoeller, Phys. Rev. Lett. **76**, 114 (1996).
[10] G. Hackenbroich, Phys. Rep. **343**, 463 (2001).
[11] O. Entin-Wohlman, A. Aharony, Y. Imry, Y. Levinson, and A. Schiller, Phys. Rev. Lett. **88**, 166801 (2002).
[12] A. Aharony, O. Entin-Wohlman, B. I. Halperin, and Y. Imry, Phys. Rev. B **66**, 115311 (2002).
[13] A. Aharony, O. Entin-Wohlman, and Y. Imry, Phys. Rev. Lett. **90**, 156802 (2003).
[14] B. Kubala and J. König, Phys. Rev. B **65**, 245301 (2002).
[15] J. König and Y. Gefen, Phys. Rev. Lett. **86**, 3855 (2001); Phys. Rev. B **65**, 045316 (2002).
[16] Z. T. Jiang, Q. F. Sun, X. C. Xie, and Y. Wang, Phys. Rev. Lett. **93**, 076802 (2004).
[17] F. Li, X. Q. Li, W. M. Zhang, and S. A. Gurvitz, EuroPhys. Lett. **88**, 37001 (2009).
[18] M. Sigrist, T. Ihn, K. Ensslin, D. Loss, M. Reinwald, and W. Wegscheider, Phys. Rev. Lett. **96**, 036804 (2006).
[19] V. I. Puller and Y. Meir, Phys. Rev. Lett. **104**, 256801 (2010).
[20] T. L. Schmidt, P. Werner, L. Muhlbacher, and A. Komnik, Phys. Rev. B **78**, 235110 (2008).
[21] X. Zheng, J. S. Jin, S. Welack, M. Luo, and Y. J. Yan, J. Chem. Phys. **130**, 164708 (2009).
[22] D. M. Kennes, S. G. Jakobs, C. Karrasch, and V. Meden, Phys. Rev. B **85**, 085113 (2012).
[23] D. Segal, A. J. Millis, and D. R. Reichman, Phys. Rev. B **82**, 205323 (2010); S. Bedkihal and D. Segal, *ibid.* **85**, 155324 (2012).
[24] M. W. Y. Tu, W. M. Zhang, and J. S. Jin, Phys. Rev. B **83**, 115318 (2011).
[25] Matisse Wei-Yuan Tu and W. M. Zhang, Phys. Rev. B **78**, 235311 (2008); M. W. Y. Tu, M. T. Lee, and W. M. Zhang, Quantum Inf. Processing (Springer) **8**, 631 (2009).
[26] J. S. Jin, M. W. Y. Tu, W. M. Zhang, and Y. J. Yan, New J. Phys. **12**, 083013 (2010).
[27] A. J. Leggett, S. Chakravarty, A. T. Dorsey, M. P. Fisher, A. Garg, and W. Zwerger, Rev. Mod. Phys. **59**, 1 (1987).
[28] H. Haug and A.-P. Jauho, in *Quantum Kinetics in Transport and Optics of Semiconductors*, Springer Series in Solid-State Sciences, 2nd ed. (Springer-Verlag, Berlin, 2008), Vol. 123.
[29] Note that since we consider only noninteracting electrons, the phase rigidity is held for arbitrary biases. When a high bias is applied, the steady-state current can break phase rigidity due to electron-electron interactions.[30]
[30] B. Spivak and A. Zyuzin, Phys. Rev. Lett. **93**, 226801 (2004).
[31] Such an occupation symmetry was first found in other systems we have recently studied; see H. N. Xiong, W. M. Zhang, M. W. Y. Tu, and D. Braun, Phys. Rev. A **86**, 032107 (2012). This occupation symmetry can also be obtained through a SU(2) transformation given in Ref. [17]. Also note that though the definition of A_- involves the gauge degree of freedom χ, the occupation, $\langle A_-^\dagger A_-\rangle$, is gauge invariant.